Broadly cross-reactive antibodies dominate the human B cell response against 2009 pandemic H1N1 influenza virus infection

Jens Wrammert,[1,2] Dimitrios Koutsonanos,[2] Gui-Mei Li,[1,2] Srilatha Edupuganti,[4,5] Jianhua Sui,[6] Michael Morrissey,[8] Megan McCausland,[1,2] Ioanna Skountzou,[2] Mady Hornig,[9] W. Ian Lipkin,[9] Aneesh Mehta,[3] Behzad Razavi,[5] Carlos Del Rio,[3,4,10] Nai-Ying Zheng,[8] Jane-Hwei Lee,[8] Min Huang,[8] Zahida Ali,[8] Kaval Kaur,[8] Sarah Andrews,[8] Rama Rao Amara,[1,2] Youliang Wang,[1] Suman Ranjan Das,[11] Christopher David O'Donnell,[12] Jon W. Yewdell,[11] Kanta Subbarao,[12] Wayne A. Marasco,[6] Mark J. Mulligan,[4] Richard Compans,[1] Rafi Ahmed,[1,2] and Patrick C. Wilson[8]

[1]Emory Vaccine Center, [2]Department of Microbiology and Immunology, [3]Division of Infectious Diseases, Department of Medicine, School of Medicine, Emory University, Atlanta, GA 30322
[4]Hope Clinic of the Emory Vaccine Center, School of Medicine, Division of Infectious Disease, Decatur, Georgia, 30030
[5]Department of Internal Medicine, Emory University, Atlanta, GA 30322
[6]Department of Cancer Immunology and AIDS, Dana-Farber Cancer Institute
[7]Department of Medicine, Harvard Medical School, Boston, MA 02115
[8]Department of Medicine, Section of Rheumatology, The Committee on Immunology, The Knapp Center for Lupus and Immunology Research, The University of Chicago, Chicago, IL 60637
[9]Center for Infection and Immunity, Columbia University Mailman School of Public Health, New York, NY 10032
[10]Hubert Department of Global Health, Rollins School of Public Health and Department of Medicine, Emory University School of Medicine, Atlanta, GA 30322
[11]Laboratory of Viral Diseases, [12]Laboratory of Infectious Diseases, National Institute of Allergy and Infectious Diseases, Bethesda, MD 20892

The 2009 pandemic H1N1 influenza pandemic demonstrated the global health threat of reassortant influenza strains. Herein, we report a detailed analysis of plasmablast and monoclonal antibody responses induced by pandemic H1N1 infection in humans. Unlike antibodies elicited by annual influenza vaccinations, most neutralizing antibodies induced by pandemic H1N1 infection were broadly cross-reactive against epitopes in the hemagglutinin (HA) stalk and head domain of multiple influenza strains. The antibodies were from cells that had undergone extensive affinity maturation. Based on these observations, we postulate that the plasmablasts producing these broadly neutralizing antibodies were predominantly derived from activated memory B cells specific for epitopes conserved in several influenza strains. Consequently, most neutralizing antibodies were broadly reactive against divergent H1N1 and H5N1 influenza strains. This suggests that a pan-influenza vaccine may be possible, given the right immunogen. Antibodies generated potently protected and rescued mice from lethal challenge with pandemic H1N1 or antigenically distinct influenza strains, making them excellent therapeutic candidates.

CORRESPONDENCE
Rafi Ahmed:
rahmed@emory.edu
OR
Patrick C. Wilson:
wilsonp@uchicago.edu

Abbreviations used: GC, germinal center; HA, hemagglutinin; HAI, hemagglutinin inhibition; MN, microneutralization; TCID50, 50% tissue culture infectious dose.

Influenza is the seventh leading cause of death in the United States (Beigel, 2008), with the elderly, the very young, pregnant women, and otherwise immune-compromised populations accounting for >90% of influenza-related deaths. The pandemic H1N1 influenza virus strain is immunologically distinct from other influenza viruses, leaving large population groups susceptible to infection (Brockwell-Staats et al., 2009; Dawood et al., 2009; Garten et al., 2009;

The Rockefeller University Press $30.00
J. Exp. Med. Vol. 208 No. 1 181-193
www.jem.org/cgi/doi/10.1084/jem.20101352

The Journal of Experimental Medicine

Hancock et al., 2009). The Centers for Disease Control reports that there were an estimated 60 million cases of the 2009 H1N1 pandemic strain, which caused ∼256,000 hospitalizations. An unusually high frequency of severe disease occurred in younger and otherwise healthy patients (Hancock et al., 2009). In addition, rare infections with avian H5N1 influenza strains in humans had close to a 50% mortality rate (Subbarao and Joseph, 2007). Emergence of a zoonotic or antigenically distinct strain that combined even a fraction of the morbidity and mortality of the pandemic H1N1 and H5N1 viruses would have dire consequences. Antibodies play a key role in protection against influenza infection in vivo (Puck et al., 1980; Gerhard et al., 1997; Luke et al., 2006; Simmons et al., 2007). The fact that there were little or no preexisting antibody titers present before the emergence of this pandemic virus, and that the virus atypically caused such severe disease in young adult, illustrates the importance of comprehensively understanding the B cell responses and antibody specificities induced by infection with this influenza virus.

Here, we have analyzed the plasmablast responses induced by pandemic H1N1 infection and generated a panel of monoclonal antibodies (mAbs) from these cells to analyze their characteristics in detail. In contrast to seasonal vaccination, we show that a majority of the neutralizing antibodies induced by infection were broadly cross-reactive with all recent annual H1N1 strains, as well as the highly pathogenic 1918 H1N1 and avian H5N1 strains. These neutralizing antibodies bound predominantly to conserved epitopes in the hemagglutinin (HA) stalk region (Ekiert et al., 2009; Sui et al., 2009), with some binding to novel epitopes in the HA globular head. The high frequency of these HA-stalk binding antibodies is of particular interest, as this epitope is a promising target for a broadly protective influenza vaccine (Steel et al., 2010). Furthermore, the cross-reactive antibodies carried highly mutated immunoglobulin genes, indicative of extensive affinity maturation. Together, these findings support a model in which infection predominantly activated broadly cross-reactive memory B cells that then underwent further affinity maturation. We propose that the expansion of these rare types of memory B cells may explain why most people did not become severely ill, even in the absence of preexisting protective antibody titers. Recent studies in mice strongly support the idea that consecutive immunizations with antigens from divergent influenza stains can indeed hone the antibody response to preferentially target broadly protective conserved epitopes (Wang et al., 2010; Wei et al., 2010). Our findings demonstrate that cross-reactive antibodies can be preferentially induced in humans given the right immunogen, providing further support for the feasibility of generating a pan-influenza vaccine. Finally, in vivo challenge experiments showed that the neutralizing antibodies isolated protected mice challenged with a lethal dose of pandemic H1N1 influenza virus, even when administered therapeutically 72 h after infection, and also provided protection against antigenically distinct H1N1 influenza strains. These antibodies are thus promising as therapeutics against pandemic H1N1, as well as most other H1N1 and H5N1 influenza strains, especially in high-risk populations such as immunosuppressed patients and the elderly.

RESULTS

Influenza-specific plasmablasts are persistently induced throughout infection, providing a rich source of antiviral mAbs

B cell responses were examined in nine patients infected with the pandemic 2009 H1N1 influenza virus. These patients had varying courses and severity of disease. The cases ranged from mild disease with rapid viral clearance within a few days after onset of symptoms to severe cases that shed virus for several weeks and required hospitalization with ventilator support. A majority of the patients were treated with antiviral drugs. The diagnoses were confirmed by pandemic H1N1-specific RT-PCR and serology. All patients had neutralizing titers of serum antibodies at the time of blood collection. A summary of the clinical patient data are shown in Table I. The majority of samples were obtained around 10 d after the onset of symptoms, with the exception of a particularly severe case where sampling was done 31 d after symptom onset.

Antigen-specific plasmablasts appear transiently in peripheral blood after vaccination with influenza or other vaccines (Brokstad et al., 1995; Bernasconi et al., 2002; Sasaki et al., 2007; Wrammert et al., 2008), but the kinetics of their appearance and persistence during an ongoing infection remain unclear. Here, we have analyzed the magnitude and specificity of the plasmablast response in blood samples taken within weeks after onset of clinical symptoms of pandemic H1N1 influenza virus infection. Using a virus-specific ELISPOT assay, it was possible to show a significant number of pandemic H1N1-reactive plasmablasts in the blood of the infected patients, whereas none were detectable in a cohort of healthy volunteers (Fig. 1, A and B). These cells were also readily detectable several weeks after symptom onset in the more severe cases. Fig. 1 (A and C) illustrates that, of the total IgG-secreting cells, over half of the cells were producing antibodies that bound pandemic H1N1 influenza virus. Moreover, plasmablasts specific for HA occurred at 30–50% the frequency of virus-specific cells (Fig. 1, C and D), the specificity most likely to be critical for protection. Most patients also had a relatively high frequency of plasmablasts, forming antibodies that bound to past, seasonal influenza strains (Fig. 1 C) or recombinant HA from the previous annual H1N1 strain, A/Brisbane/59/2007. Based on the overall frequency of pandemic H1N1-specific cells, it is likely that the cells binding other strains were overlapping populations and cross-reactive. None of the induced plasmablast cells bound to recombinant HA from the H3N2 strain from the same vaccine (A/Brisbane/10/2007). These findings demonstrate that influenza-specific human plasmablasts are continuously generated throughout an ongoing infection and that a fairly high proportion of these cells make antibodies that also cross-react with previous annual H1N1 influenza strains.

To analyze the specificity, breadth, and neutralizing capacity of these plasmablasts, we used single-cell PCR to amplify the heavy and light chain variable region genes from individually

sorted cells (defined as $CD19^+$, $CD20^{lo/-}$, $CD3^-$, $CD38^{high}$, $CD27^{high}$ cells; Fig. 1 E; Wrammert et al., 2008; Smith et al., 2009). These genes were cloned and expressed as mAbs in 293 cells, and the antibodies were screened for reactivity by ELISA. Thresholds for scoring antibodies as specific to the influenza antigens were empirically determined based on being two standard deviations greater than the background level of binding evident from 48 naive B cell antibodies (Fig. S1 A). Of 86 antibodies generated in this fashion, 46 (53%) bound pandemic H1N1 (Fig. 1 F) and one third (15 antibodies) were reactive to HA (Fig. 1 G and Fig. S2 A), most of them at sub-nanomolar avidities (based on surface plasmon resonance analyses; Fig. S2 B). On a per donor basis, 55% of the mAbs bound to purified pandemic H1N1 virions (range: 33 to 77%). Of the virus-specific antibodies, 31% bound to recombinant HA (range: 14 to 55%). We conclude that virus-specific plasmablasts are readily detected after pandemic H1N1 influenza virus infection and that virus-specific human mAbs can be efficiently generated from these cells.

Plasmablasts from patients infected with pandemic H1N1 influenza were highly cross-reactive to prepandemic influenza strains

As the plasmablasts are specifically induced by the ongoing immune response, we can learn about the origin of the B cells activated by pandemic H1N1 infection. Consistent with the frequency of plasmablasts secreting antibodies binding annual influenza strains by ELISPOT analyses (Fig. 1 C), a majority (29/46, or 63%) of the pandemic H1N1-specific antibodies also cross-reacted with seasonal influenza viruses (Fig. 2, A and B). In fact, by ELISA, one third of these antibodies bind to the prepandemic strains at lower concentrations than they did to the pandemic H1N1 strain, suggesting higher avidity binding. By comparison, only 22% (11/50) of plasmablasts induced by annual H1N1 strains before the pandemic could bind the pandemic H1N1 influenza (Fig. S1 B). We propose that the cross-reactivity of pandemic H1N1-induced cells derives from the activation of memory cells originally specific for past influenza immunizations in an original antigenic sin fashion.

Evidence of extensive affinity maturation suggests a high frequency of memory cell activation against the pandemic H1N1 strain

Based on the 10–15-fold induction of plasmablasts and expression of intracellular Ki67 during ongoing immune responses (Brokstad et al., 1995; Bernasconi et al., 2002; Sasaki et al., 2007; Smith et al., 2009; Wrammert et al., 2008), we can assume that most plasmablasts result from the ongoing infection

Table I. Summary of clinical data for patients with acute pandemic H1N1 virus infections

Patient	Age	Gender	HAI titer	MN titer	Co-morbidities	Initial symptoms	Hospital course	Sample collection	Antiviral treatment	mAb
EM	30	F	640	1280	none	Fever, cough, dyspnea	Acute respiratory distress syndrome, bacterial pneumonia, pulmonary embolism, prolonged oscillatory ventilator support, tracheostomy, discharged after 2 mo	Day 31	Oseltamivir	Yes
1000	37	M	80	40	Hypertension, interstitial lung disease of unknown etiology	Fever, cough, shortness of breadth, nausea, vomiting	Pneumonia, acute sinusitis, acute renal failure, discharged after 8 d	Day 18	Oseltamivir, Zanamavir	Yes
70	38	F	80	160	none	Fever, cough, body aches	N/A	Day 15	None	Yes
1009	21	M	20	20	Congenital heart disease, repair for Tetralogy of Fallot	Fever, cough, sore throat, nausea, diarrhea	N/A	Day 9	Oseltamivir	Yes
1010	24	M	10	10	none	Fever, cough, nausea, vomiting diarrhea	N/A	Day 11	Oseltamivir	No
1011	25	M	20	10	none	Fever, cough, sore throat, vomiting, headache, confusion	N/A	Day 9	Oseltamivir	No
1013	26	M	80	160	none	Fever, cough, sore throat, body aches, nausea, vomiting, diarrhea	N/A	Day 9	None	No
1014	45	F	80	20	none	Fever, chills, cough, sore throat, body aches, headache, nausea, vomiting	N/A	Day 9	None	No

The mAb column indicates whether mAbs were made from the plasmablasts of these patients.

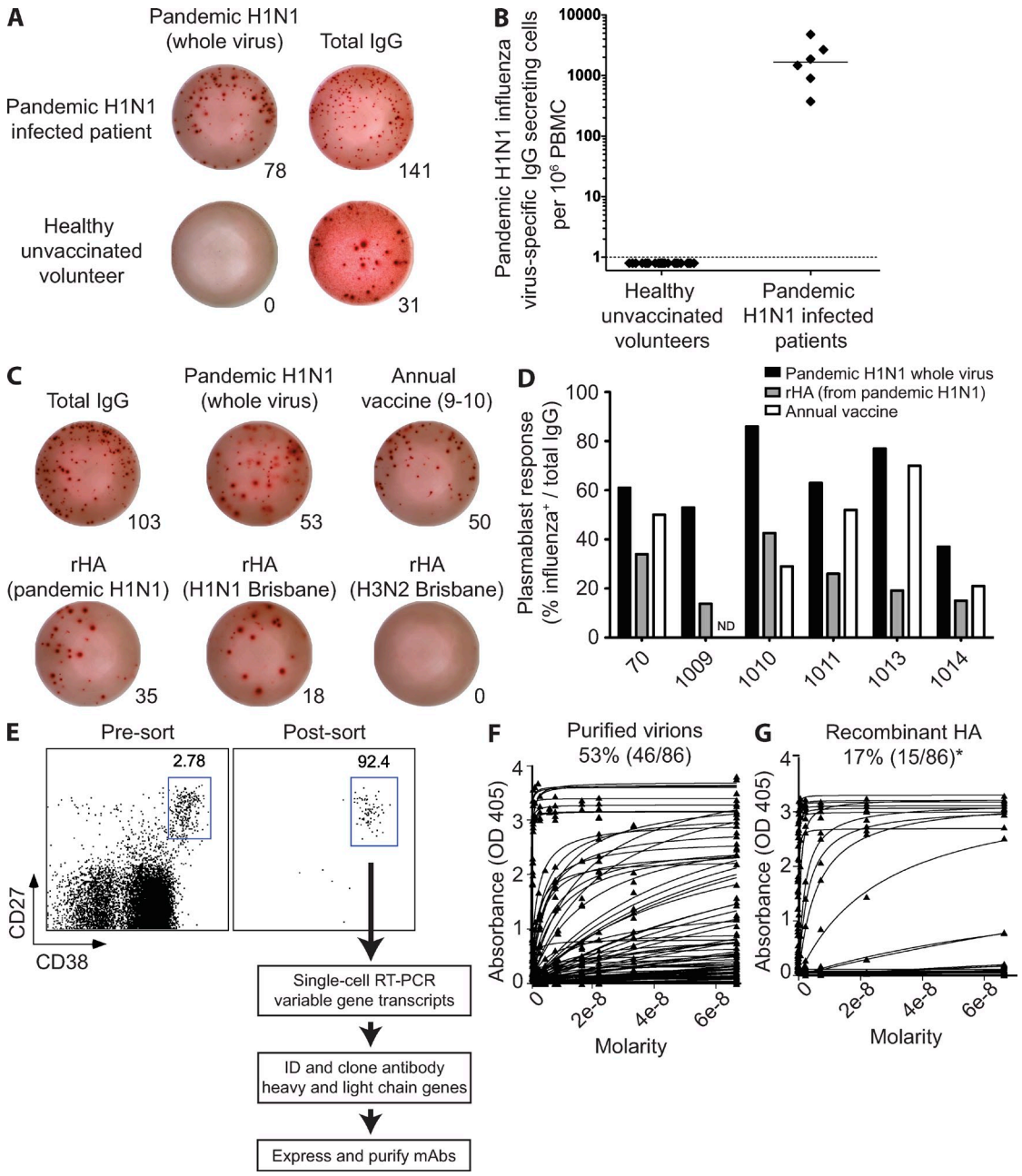

Figure 1. Generation of human mAbs against pandemic H1N1 influenza virus from infected patients. (A and B) Magnitude of the plasmablast response observed in peripheral blood of six pandemic H1N1-infected patients and 22 healthy (noninfected/nonvaccinated) donors by ELISPOT analysis. (A) Representative ELISPOT. Numbers of plasmablasts secreting antibody reactive to pandemic H1N1 is compared with the total number of IgG-secreting cells from each PBMC sample (numerals). All ELISPOT assays were performed in duplicate. (B) Summary of all the donors analyzed; each dot represents one patient or control. (C and D) Specificity of the sorted plasmablasts measured by ELISPOT analysis. Representative ELISPOT showing plasmablasts producing antibodies reactive with total IgG or pandemic H1N1 whole virus, annual influenza vaccine (2009/2010 TIV vaccine), or recombinant HA from pandemic H1N1, the previous year's annual vaccine H1N1 strain (A/Brisbane/59/2007), or the previous years H3N2 strain (A/Brisbane/10/2007). (D) Summary of the frequency of whole IgG secreting cells specific to pandemic H1N1 whole virus, recombinant HA from pandemic H1N1, and recombinant HA from the previous year's vaccine. Donors EM1 and SF1000 were not analyzed in this fashion, as the antigens were not available for live-cell analyses at that time point in the pandemic. (E) Sorting of plasmablast cells from pandemic H1N1 influenza–infected patients to generate mAbs. Flow cytometry plots show the percentage of $CD27^{hi}CD38^{hi}$ cells (dot plots are gated on $CD3^{-}CD20^{lo/-}$ lymphocytes). The plasmablasts are defined herein as $CD3^{-}CD20^{lo/-}CD19^{+}CD38^{hi}CD27^{hi}$ cells. (right) An example of post-sort purity of ungated cells (verified for each sample). Single plasmablasts were isolated from the sorted fraction by cell sorting, and variable antibody genes were cloned from individual cells (see Materials and methods). (F and G) Scatchard plots of binding of the isolated mAbs to pandemic H1N1 whole-purified virus (F) and pandemic H1N1 recombinant HA (G) as measured by ELISA. Antibodies were scored positive (frequency above plots) if they bound at least two standard deviations greater than the mean absorbance of naive B cell antibodies at 10 µg/ml (detailed in Fig. S1 A).

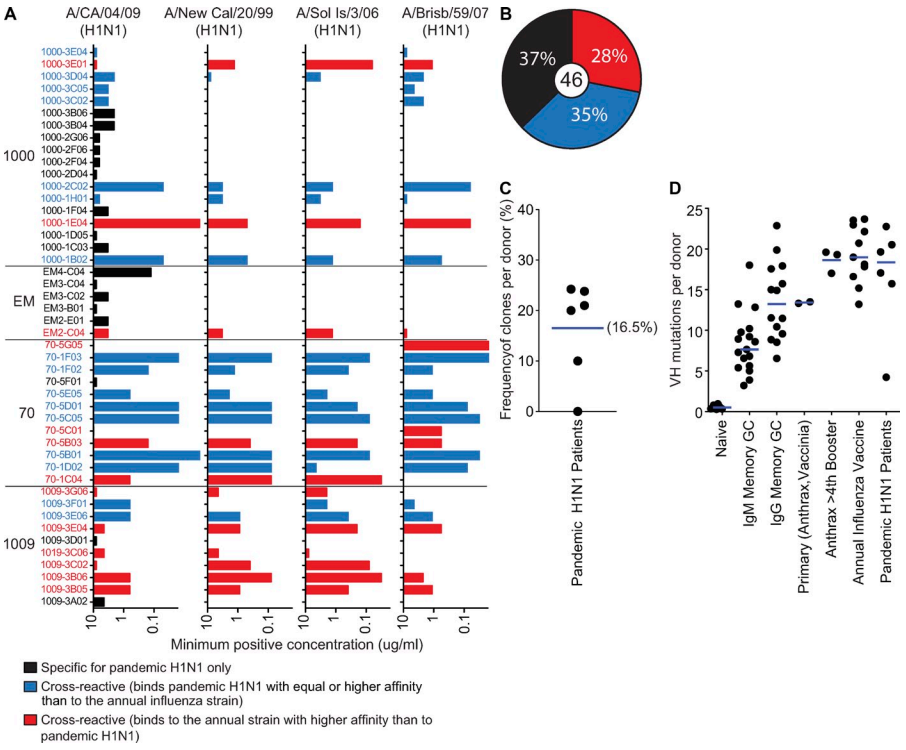

Figure 2. Plasmablasts induced by pandemic H1N1 infection are highly cross-reactive and have accumulated particularly high levels of variable gene somatic hypermutation. (A and B) Pandemic H1N1 reactive mAbs isolated from infected patients (1000, EM, 70, 1009) were assayed for binding to annual H1N1 influenza strain whole virus. The minimum detectable concentration is defined as two standard deviations above the mean binding of 48 randomly chosen naive B cell antibodies (Fig. S1 A). Bars are color coded to approximate levels of cross-reactivity to the annual vaccine (circulating) strains of recent years. Panels A and B use the same color scheme. Each value is representative of at least two replicate ELISAs repeated until a single consistent minimum concentration was established. The center numeral equals total antibodies. (C) Analysis of the variable gene sequences from plasmablasts of the four pandemic H1N1-infected patients indicated that ~16.5% of the pandemic H1N1-induced plasmablasts were clonally related (shared identical VH and JH genes and CDR3 junctions). (D) The average number of somatic hypermutations in the pandemic H1N1 patient plasmablast variable region genes compared with primary IgG plasmablast responses to vaccinia (small pox) or the anthrax vaccine, or after at least 4 boosters with the anthrax vaccine. To account for the obvious outlier in the pandemic H1N1 group (patient-EM), median values are indicated by the bar. Student's *t* tests excluding the outlier indicated a p-value of <0.04 for the remaining five pandemic H1N1 samples compared with the IgG memory and germinal center (GC) cells or the primary IgG plasmablast responses (0.2 with EM included) and a p-value of <0.0001 against the IgM populations. Notably, besides patient EM, each individual set of VH genes averaged significantly more mutations than the IgG memory and GC or the primary responses (Fig. S3 A). Each point represents one individual donor and is averaged from 25–75 sequences, except for the primary response to anthrax from which only 10 VH genes could be cloned from single cells because of the highly limited response. Mutations accumulated per individual sequence are depicted in Fig. S3. Detailed sequence characteristics are provided in Tables S1–S3. The naive, IgG and IgM GC and memory populations are derived from historical data (Zheng et al., 2004, 2005; Koelsch et al., 2007; Wrammert et al., 2008).

or vaccine response. The ready detection of clonal expansions at a mean frequency of 16.5% of the cells for the six patients supports this view (based on CDR3 sequence similarity; Fig. 2 C). Since the discovery of somatic mutation, it has been appreciated that mutations progressively accumulate on variable genes after repeated immunizations (McKean et al., 1984). Thus, we can gain insight into the origin of the pandemic H1N1 response by comparing the somatic mutation frequency of the plasmablasts present during H1N1 infection to that of other plasmablast responses. The PCR strategy allowed isolation of either IgG or IgA transcripts and identified 68% IgG and 32% IgA plasmablasts from the patients. Similar to plasmablasts induced by annual vaccination (Wrammert et al., 2008), or after a fourth booster vaccine to anthrax, the variable genes of novel H1N1-induced cells from five of the six patients harbored high numbers of somatic mutations (averaging >19 per patient; Fig. 2 D and Fig. S3 A). For these 5 patients, mutations had accumulated significantly more than from primary IgG plasmablast responses to anthrax or vaccinia (small pox) vaccines, and more so than for IgG-positive memory B cells from our historical data that averaged 14/VH gene (Student's *t* test $P < 0.05$; Zheng et al., 2004, 2005; Koelsch et al., 2007; Wrammert et al., 2008; Fig. 2 C and Fig. S3 B) or from 347 IgG memory cell sequences previously published by another group (averaging 15/VH gene; de Wildt et al., 2000). Interestingly, for patient EM (outlier in Fig. 2 D) who had the most severe infection (Table I), mutations had accumulated at a significantly lower frequency than the IgG controls (Fig. S3 A; $P < 0.0001$), suggesting a unique circumstance such as a low-level or lacking primary response. Detailed sequence characteristics for pandemic H1N1-induced plasmablasts are provided in Tables S1–S3. Though based on a limited

Antibodies were tested at 10 µg/ml and threefold serial dilutions until a nonbinding concentration was determined. Each antibody was tested in at least two (and typically more) replicates for specificity and affinity estimations. Note that only 14 of 15 HA-binding antibodies have curves in G because one of the HA-reactive antibodies only binds HA on whole virions, not on the recombinant protein.

number of patients, the frequent cross-reactivity and high number of somatic mutations support a model in which many of the plasmablasts induced by pandemic H1N1 infection arose from cross-reacting memory B cells.

A majority of the neutralizing antibodies bound to highly conserved epitopes in both the HA stalk and head regions

A high frequency of the HA-specific antibodies was able to neutralize the virus in vitro (totaling 73% or 11/15; Fig. 3 A). These neutralizing antibodies could be further categorized into two distinct groups: (a) neutralizing antibodies that displayed hemagglutination inhibition (HAI) activity (HAI^+) and (b) neutralizing antibodies that had no HAI activity, indicating that they bound to sites other than the HA active site. Interestingly, antibodies of the latter type were predominant in the response (Fig. 3 A). This specificity is reminiscent of antibodies against the recently discovered broadly neutralizing epitopes found on the HA stalk, rather than those located on the HA globular head that is more typical for neutralizing antibodies (Ekiert et al., 2009; Sui et al., 2009). Importantly, five of these antibodies are indeed of similar specificity (including antibodies 70-5B03, 70-1F02, 1000-3D04, and a clonal pair from donor 1009: 3B05 and 3E06). These five antibodies bind with high affinity to most H1 strains including all from the vaccines of the past 10 yr, the 1918 pandemic strain, and to the H5 of a highly pathogenic

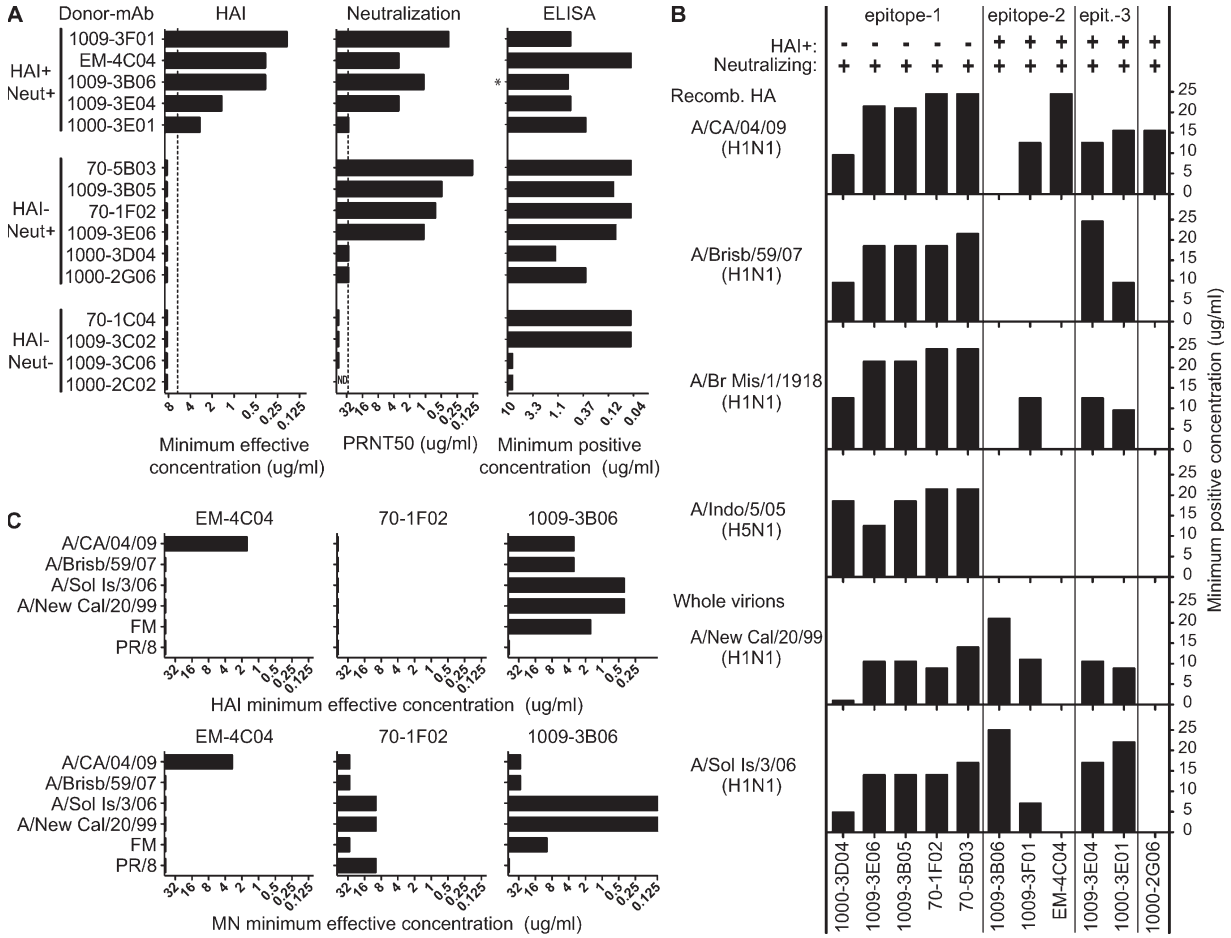

Figure 3. HA-specific antibodies induced by pandemic H1N1 infection bind cross-reactive neutralizing epitopes. (A) In vitro functional analysis of 15 antibodies from indicated patients that bound pandemic H1N1 influenza recombinant HA protein. The left panel shows HAI minimum effective antibody concentration, the middle panel shows PRNT50 plaque reduction neutralization minimum effective antibody concentration, and the right panel shows ELISA binding summarized as minimum positive concentration (as defined for Fig. 2) against recombinant HA (original curves are in Fig. 1 F and Fig. S2 A). The antibodies are grouped based on whether they show HAI and/or neutralizing (neut) function. Antibody 1009-3B06 was only tested for binding to whole virus, as this antibody did not bind to rHA due to binding of a quaternary or conformationally sensitive epitope that is not present in the recombinant protein. HAI and neutralization assays were performed in duplicate and repeated at least three times. ELISA curves are provided in Fig. S2 A. (B) ELISA binding as shown by minimum positive concentration (defined for Fig. 2) of neutralizing mAbs to rHA or whole virions from pandemic H1N1 or other influenza strains (ELISA binding curves are provided in Fig. S2 A). Three binding patterns (epitopes 1 and 2, and 3) were observed that coincided with specificity comparisons by competitive ELISA, as illustrated in Fig. 4 A. (C) Three representative neutralizing antibodies (EM-4C04, 70-1F02, and 1009-3B06) were used for HAI and microneutralization (MN) activity against pandemic H1N1 and several other annual or laboratory H1N1 influenza strains. Experiments were performed in duplicates and repeated at least three times. Minimum effective concentration is shown for both assays.

avian influenza strain (Fig. 3 B and Fig. S2 A). In addition, these five antibodies cross-compete for a similar epitope that was not over-lapping with the HAI$^+$ antibodies (Fig. 4 A, epitope-1). These antibodies are competitively inhibited by a commercial antibody referred to as C179 that binds this HA stalk region (Okuno et al., 1993), and four of five of these antibodies are encoded by the hallmark VH1-69 gene (Ekiert et al., 2009; Sui et al., 2009). To verify HA stalk reactivity, these five antibodies were tested for binding to H5 variants predicted to affect the stalk epitope by the crystal structure, and their binding patterns were compared with that of the prototypical stalk antibody (mAb F10; Sui et al., 2009; Fig. 4 B). Each H5 variant has a single residue mutation in the stalk region and was transiently expressed on 293T cells. FACS analysis showed that the five antibodies bound to all 13 H5 variants tested at levels quite similar to F10, for which a crystal structure had been generated to define this epitope. Thus, half of the neutralizing and a surprising 10% of all antibodies induced by pandemic H1N1 infection bound to a conserved, critical epitope on the HA stalk. By comparison, none of 50 H1N1 strain-specific antibodies that we had previously isolated after annual vaccination before the 2009 pandemic had this reactivity (unpublished data). The frequency of pandemic-induced, stem-reactive antibodies (5/46) versus those from annual vaccine (0/50) is significantly greater (Chi-square test, $P = 0.02$). Further, this specificity is only rarely seen in human memory B cells (Corti et al., 2010) or from phage-display libraries (Sui et al., 2009). These observations support

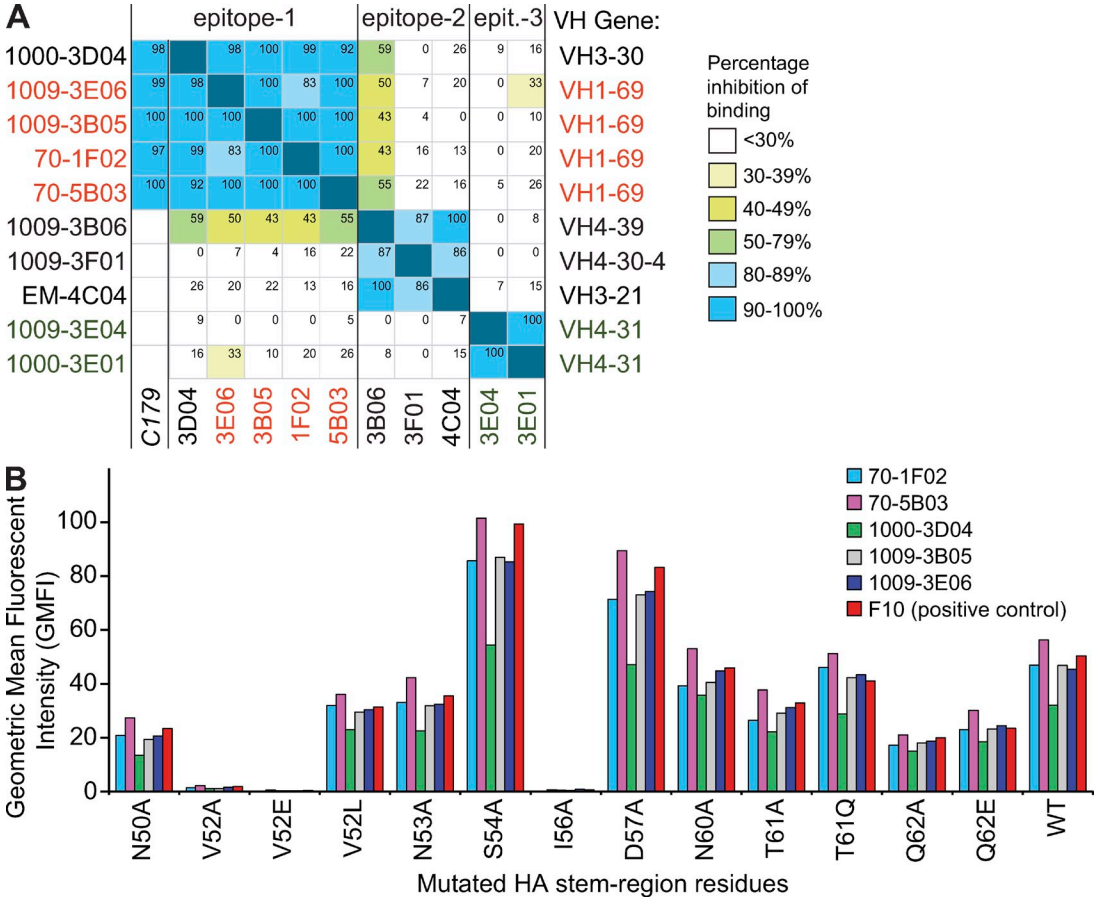

Figure 4. The neutralizing antibodies bind to three nonoverlapping epitopes in either the stalk or the globular head of the HA molecule. (A) Competition ELISA assays were used to determine the similarity in specificity between the various neutralizing antibodies. Shown is the percentage of competition of each antibody in an ELISA binding assay against all other neutralizing antibodies. A 10-fold molar excess of unlabeled antibody was used to inhibit a biotinylated antibody. Percent competition is calculated as the reduction in absorbance relative to the level of inhibition of any particular antibody against itself. Colors indicate degree of inhibition of antibody binding, as indicated. Antibody C179 is a commercial antibody that binds to the stalk region of the HA molecule identifying epitope-1. Epitope-2 and -3 are each on the HA-head active site. 1000-2G06 and the nonneutralizing, but HA-binding, antibodies had no competition with any of the other HA-reactive antibodies and are therefore not shown. VH gene usage of the individual antibodies is listed on the right. All assays were performed in duplicate. (B) Plasmids encoding full-length WT H5-TH04 (A/Thailand/2-SP-33/2004 [H5N1]) and its mutants were transiently transfected into 293T cells. 24 h after transfection, cells were harvested for FACS analysis, and binding of indicated antibodies was tested at 10 µg/ml. The cell surface HA expression of each of the mutants were verified with a ferret anti-H5N1 serum (not depicted). Antibody F10 was one of the antibodies used to characterize the HA stalk epitope by x-ray crystallography (Sui et al., 2009) and served as a positive control for the binding pattern expected of HA stalk–reactive antibodies to these HA mutants.

the idea that a vaccine might be developed that preferentially targets the HA stalk, thus providing broad protection against many influenza strains.

The remaining neutralizing antibodies were HAI^+ and therefore bound to the HA globular head. Based on cross-competition analyses, these antibodies fell into two groups binding nonoverlapping regions of the HA head, including epitope-2 and epitope-3 (Fig. 3 B and Fig. 4 A). Indeed, using spontaneous escape mutant selection, we found that the EM4C04 mAb binds to the Sa region of the HA globular head (unpublished data). Thus, by proximity based on the competition assay (Fig. 4 A), we can predict that all of the epitope-2 antibodies bind near the Sa/Sb region (including EM-4C04, 1009-3B06, and 1009-3F01).

Broadly reactive antibodies binding both pandemic H1N1 strains and common annual H1N1 strains have been identified both in humans (Krause et al. 2010; Xu et al., 2010) and in mice (Manicassamy et al., 2010). It is notable that three of five of the HA globular-head–binding antibodies induced by pandemic H1N1 infection were also broadly reactive to various H1N1 strains (Fig. 3 B). One such novel antibody was the SF1009-3B06 antibody that reacts strongly with the pandemic H1N1 strain, as well as all recent H1N1 vaccine strains (Fig. 3 B and Fig. S2 A). The precise epitope to which the 1009-3B06 antibody binds appears to be quite unique; it is only accessible on whole virions, not on recombinant HA, suggesting that the epitope is quaternary in nature. Finally, two antibodies cross-reacted and inhibited hemagglutination to all recent H1 vaccine strains and reacted strongly to the 1918 pandemic strain (antibodies 1009-3E04 and 1000-3E01; Fig. 3 B and Fig. 4 A, epitope-3). These mAbs bind to past vaccine strains with higher avidity than to the pandemic H1N1. Further studies are underway to precisely identify the epitopes of all neutralizing antibodies in this study.

Only two of 11 neutralizing antibodies were highly specific for the pandemic H1N1 strain alone (Fig. 3 B and Fig. S2 A), including a low avidity antibody, 1000-2G06, which only showed slight neutralization capacity in vitro, and EM-4C04, which was very effective at neutralizing the pandemic H1N1 influenza. We conclude from these experiments that a surprising 82% (9/11) of the neutralizing plasmablasts that we isolated during pandemic H1N1 influenza infections were broadly cross-reactive to multiple influenza strains.

Potent in vivo protection and rescue of mice challenged with a lethal dose of pandemic H1N1 or antigenically distinct influenza virus strains

There is a distinct interest in developing monoclonal antibodies for use in a therapeutic setting. We selected three representative antibodies of the set we have identified for detailed functional analysis both in vitro (Fig. 3 C) and in vivo (Fig. 5 and Fig. 6), including: EM-4C04, 1009-3B06, and 70-1F02. The antibodies EM-4C04 and 1009-3B06 are specific for the active site of the HA molecule, whereas 70-1F02 binds to the stalk region. Furthermore, EM-4C04 is highly specific for pandemic H1N1, whereas 1009-3B06 and 70-F02 display

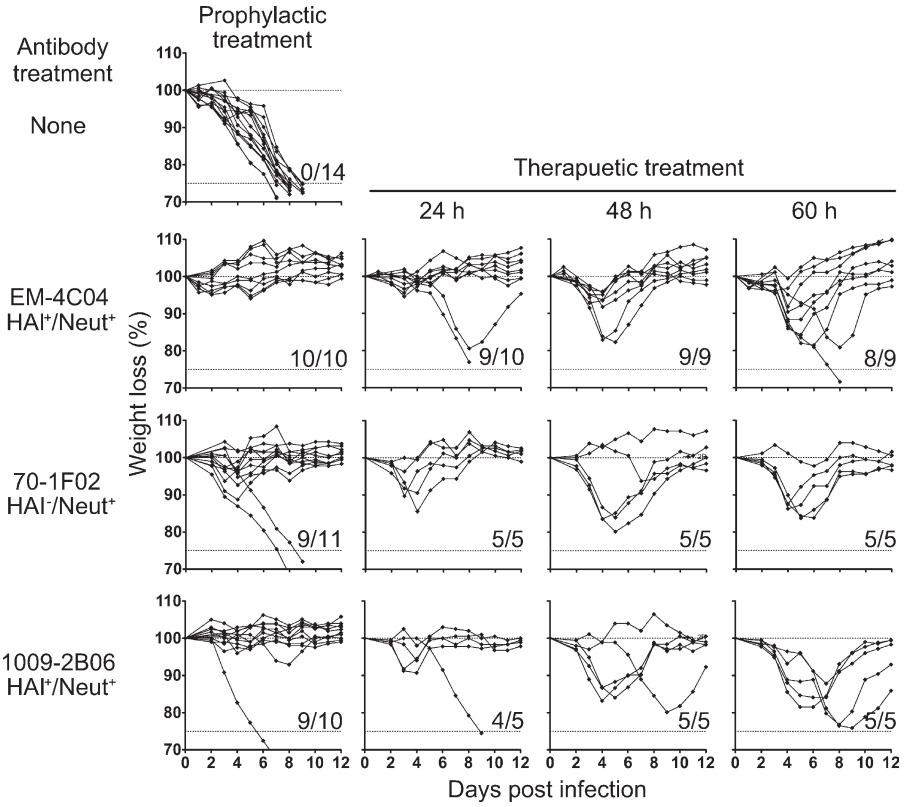

Figure 5. In vivo prophylactic and therapeutic efficacy of human mAbs against pandemic H1N1 influenza virus. 6–8-wk-old BALB/c mice were infected with a 3xLD50 dose of highly pathogenic, mouse-adapted 2009 pandemic H1N1 influenza (A/California/04/09). 24, 48, and 60 h after infection, 200 µg (10 mg/kg of body weight) of EM-4C04, 70-F02, or 1009-3B06 human mAb were injected intraperitoneally. All mice were monitored daily for body weight changes and any signs of morbidity and mortality. Percentage of initial body weight is plotted, and the number of surviving mice is shown in the lower right of each plot. Infected, untreated mice showed clear signs of sickness around day 4–5 after infection and perished by day 8–9. Prophylactic treatment is shown on the left for comparison. Antibody treatment conferred significant protection as determined by comparison of weights in untreated versus prophylaxis and at the time of treatment versus 12 d after infection (unpaired, two-tailed Student's *t* test, $P < 0.05$). The log-rank test indicated significant survival as well ($P < 0.001$). Figure shows one representative experiments of at least three independent repeat experiments.

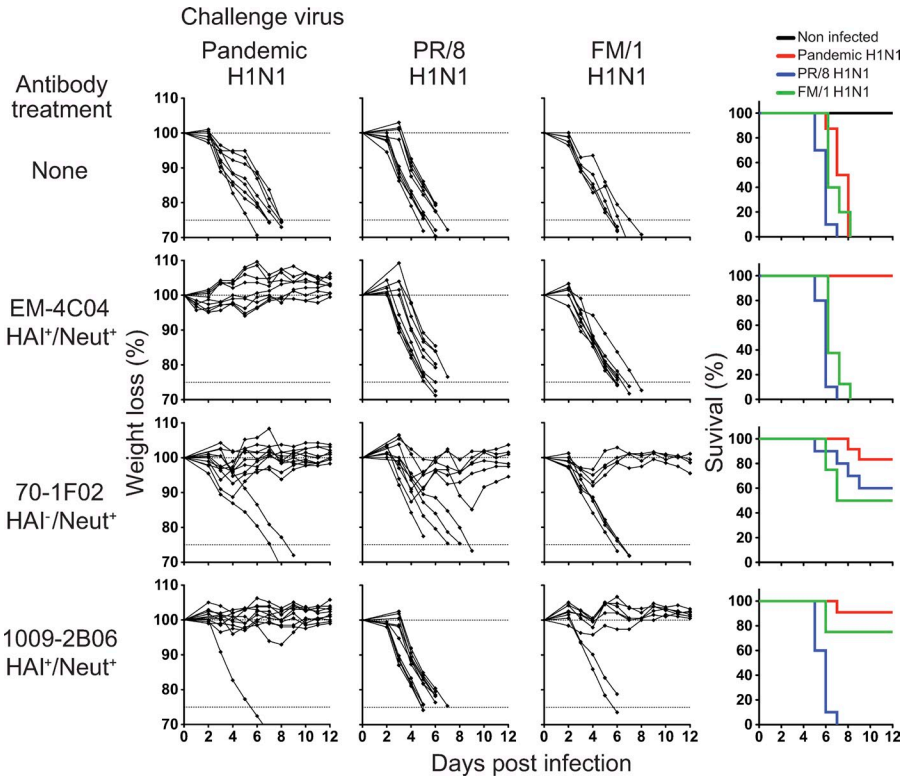

Figure 6. Breadth of in vivo prophylactic efficacy in mice. 6–8-wk-old BALB/c mice were treated with 200 µg (10 mg/kg of body weight) EM-4C04, 70-1F02, or 1009-3B06 human mAb intraperitoneally. Control mice were treated with PBS only, a control mAb or polyclonal human IgG. 12 h later, they were challenged with a 3xLD50 dose of mouse adapted pandemic H1N1, PR/8/34, or FM/1/47 influenza virus. All mice were monitored daily for body weight changes and any signs of morbidity and mortality. Percentage of initial body weight (left) and survival curves (right) are plotted. Infected, untreated mice showed clear signs of sickness ~4–5 d after infection and perished by day 8–9. Figure shows one representative experiments of at least three independent repeat experiments. Antibody treatment conferred significant protection as determined by comparison of weights in untreated versus prophylaxis, and at the time of treatment versus 12 d after infection (unpaired, two-tailed Student's *t* test, $P < 0.05$). The log-rank test indicated significant survival as well ($P < 0.003$).

broadly cross-reactive binding (Fig. 3 B) and have functional activity against multiple recent and older H1N1 strains (Fig. 3 C). These antibodies were all highly effective at providing prophylactic protection against infection with a lethal dose of mouse-adapted pandemic H1N1 in 6–8-wk-old BALB/c mice (Fig. 5). Moreover, all three antibodies were effective therapeutically, even when they were administered as late as 60 h after the lethal challenge infection, well after the mice were symptomatic. For EM-4C04, we have successfully treated mice as far out as 72 h post-infection (unpublished data). Infected mice were already showing measurable weight loss that was reversed by administration of the antibody, demonstrating therapeutic potential even after the onset of disease. Viral clearance was analyzed in mice treated at 48 h after infection with EM4C04 (Fig. S4). As early as day 4, the antibody-treated mice exhibited more than a log reduction in viral titers; titers continued to decline, such that by day 6, virus was undetectable or present at very low levels. The untreated mice perished by day 7 or 8, whereas the treated mice cleared the infection with no detectable virus on day 12. Finally, 1009-3B06 and 70-1F02, which showed activity against several current and older H1N1 seasonal influenza strains in vitro (Fig. 3 C), were also tested in vivo against antigenically distinct influenza strains. For these experiments, mice were treated with 200 µg of mAb intraperitoneally 12 h before infection with a lethal dose of either pandemic H1N1 influenza or either of the two common influenza laboratory strains PR/8/34 or FM/1/47. 1009-3B06 and 70-1F02 showed protection against these antigenically distinct H1N1 influenza strains, as illustrated in Fig. 5. EM-4C04, which is highly specific for the pandemic H1N1, had no protective effect on infection with PR/8/34 or FM/1/47. In conclusion, the antibodies characterized herein show promise for development as broadly reactive therapeutic agents against the pandemic H1N1 influenza virus, as well as against the majority of H1N1 and H5N1 influenza strains.

DISCUSSION

Our findings provide insight into the human B cell responses to a pandemic influenza virus strain. The unique genetic composition of the pandemic H1N1 influenza virus meant that our relatively young cohort probably had little or no preexisting specific antibody-mediated immunity to this virus before infection (Brockwell-Staats et al., 2009; Dawood et al., 2009; Garten et al., 2009; Hancock et al., 2009). Thus, two sources of B cells could have contributed to this response: newly recruited naive B cells and preexisting memory B cells that bound to epitopes conserved between past seasonal strains and the pandemic H1N1 strain. We theorize that predominant activation of the latter, preexisting memory cells can account for the observed high frequency of neutralizing antibodies (11/15 HA-binding antibodies), the majority (9/11) of which are cross-reactive with seasonal H1N1 strains (Fig. 3 C) and other group 1 influenza strains, including H5 HA. Several observations support this conjecture.

Most convincingly, there was a particularly high frequency of cross-reactive antibodies overall, with a high level of somatic mutations found particularly among the variable genes of cross-reacting cells (Fig. 2 and Fig. S3). In fact, by ELISA most antibodies were cross-reactive and one third of the

antibodies bound to past annual viral antigens at lower concentrations, suggesting higher avidity to past influenza strains than to the current pandemic H1N1 virus. Further, cross-reacting cells that bind with higher affinity to the pandemic H1N1 strain also have the highest frequency of variable-gene mutations (Fig. S3 B). Antibodies that were broadly cross-reactive were among the more highly mutated clones (Fig. S3 B). We propose that many of these cells were specific for cross-reactive epitopes present in annual influenza strains that then underwent further affinity maturation and adaptation to the infecting pandemic H1N1 virus. Supporting this conjecture, Corti et al. (2010) first demonstrated that naturally occurring HA stalk–reactive memory B cells could be isolated from the blood of people recently immunized with the annual vaccine, before the outbreak of pandemic H1N1. The nature of that study was to screen EBV-transformed memory cell lines, thus precluding the determination of precise frequencies of these stalk-reactive B cells. However, these antibodies were estimated to be quite rare; occurring at one in thousands to one in hundreds of influenza-binding B cells, varying by individual. In contrast, we show that plasmablasts activated by infection with the highly novel pandemic H1N1 influenza strain have substantially increased targeting to the HA stalk region epitopes, totaling 10% of all influenza-specific antibodies and half of the neutralizing antibodies (Fig. 4). In fact, most specific antibodies isolated in this study were cross-reactive to past influenza strains. Collectively, the data described supports a model in which divergent viruses that are conserved only at the most critical regions for function will elicit a higher proportion of cross-reactive and neutralizing antibodies. Thus, although the activated plasmablasts of relatively few patients could be analyzed in detail at the monoclonal antibody level, we proffer that with the proper immunogen, the long-sought development of a pan-influenza vaccine might be possible.

Interestingly, the highly specific antibody EM-4C04 was derived from a patient that had a very severe disease course, with persistent viral shedding over several weeks. In addition, the variable genes from the plasmablasts of this patient had the lowest average number of somatic mutations (Fig. 2 B, outlier, and Fig. S3 B). Collectively, the unique specificity against pandemic H1N1, the low levels of somatic mutation, and the unusually severe disease in the absence of predisposing conditions suggest that this patient may have mounted a primary immune response to the pandemic H1N1 influenza infection. The complete lack of preexisting immunity may have contributed to the more severe disease observed in this patient. In contrast, the activation of broadly cross-neutralizing memory B cells in those with immune experience to annual strains might have contributed to the less severe disease of most infected patients during the pandemic.

It is notable that there is a discrepancy between patients for serum MN titers, the severity of disease, and the frequency of plasmablasts expressing neutralizing antibodies (Table I and Fig. 3). For example, patient EM, despite having the worst disease course, had the greatest HAI and MN serum titers. This may be caused by the time from infection (day 31), allowing full seroconversion, or by the presence of highly potent antibodies, such as EM-4C04, whose activities were less likely to titer out. The highly specific nature of the response from this patient may have contributed to this advantage, ultimately better targeting the epitopes of the pandemic H1N1 strain. In contrast, patient 1009 had relatively low HAI and MN serum titers but the highest frequency of broadly neutralizing antibodies and a less severe disease course. One possibility is that our sampling from this patient was done before peak serological responses. Another possibility is that the high frequency of these potent antibodies in the memory B cell compartment may have resulted in rapid resolution of infection, precluding the development of a high serological response. A third possibility is that despite broader protection, the stalk-reactive antibodies are on the whole less potent and more rapidly titrated out than the highly specific antibodies to the HA globular head. These various possibilities will be of significant interest to study in the future.

Finally, we report the development of a large panel of human mAbs induced by pandemic H1N1 infection. Prophylactic therapy with polyclonal or mAbs has successfully been used for RSV, rabies, Hepatitis A and B, and varicella. In the case of influenza, mAbs have been shown to provide prophylactic or therapeutic protection in mice and other animal models (Reuman et al., 1983; Sweet et al., 1987; Palladino et al., 1995; Renegar et al., 2004). Passive transfer of maternal antibodies in humans has also been shown to confer protection (Puck et al., 1980). Several of the antibodies we isolated have broad neutralization capacity in vitro against divergent influenza strains and show potent prophylactic and therapeutic activity when used to treat mice that were lethally infected with influenza. These antibodies could provide much needed pandemic therapeutics to treat severe cases of influenza and to protect high-risk populations.

In conclusion, analyses of the 46 mAbs induced by pandemic H1N1 infection indicated frequent activation of broadly reactive B cells. We propose that these cells had a memory cell origin caused by cross-reactivity to conserved and functionally important epitopes. If true, it will be important to characterize the efficacy of the pandemic H1N1 vaccine to induce a similarly cross-protective response.

MATERIALS AND METHODS

Patients. All studies were approved by the Emory University, University of Chicago, and Columbia University institutional review boards (Emory IRB#22371 and 555–2000, U of C IRB# 16851E, CU IRB#AAAE1819). Patient clinical information is detailed in Table I.

PBMC and plasma isolation. All work with samples from infected patients was performed in a designated $BSL2^{+}$ facility at Emory University. Peripheral blood mononuclear cells (PBMCs) were isolated using Vacutainer tubes (BD), washed, and resuspended in PBS with 2% FCS for immediate use or frozen for subsequent analysis. Plasma samples were saved at −80°C or frozen in medium with 10% dimethyl sulfoxide for subsequent analysis.

Viruses and antigens. The pandemic H1N1 influenza virus (A/California/04/2009) was provided by R.J. Webby (St. Jude Childrens Hospital, Memphis, TN). Influenza virus stocks used for the assays were freshly grown in eggs,

prepared, and purified as previously described (Wrammert et al., 2008). The hemagglutination inhibition activity was determined using turkey red blood cells (Lampire Biological Laboratories) as previously described (Wrammert et al., 2008) or purchased as inactivated preparations (ProSpecTany TechnoGene Ltd.) which included the following: A/California/04/09 (H1N1), A/FM/1/47 (H1N1), A/PR8/34 (H1N1), A/New Caledonia/20/99 (H1N1), A/Solomon Island/3/06, A/Brisbane/59/07 (H1N1), and A/Brisbane/10/07 (H3N2). Vaccines tested included the 2006/7 vaccine from Chiron Vaccines Limited and the 2008/9 formulation from Sanofi Pasteur Inc. Recombinant HA proteins were provided by the influenza reagent resource (www.influenzareagentresource.org) of the CDC (recombinant HA from A/California/04/2009 [H1N1; #FR-180], A/Brisbane/10/2007 [H1N1; #FR-61], A/Brisbane/59/2007 [H3N2; #FR-65]) or by Biodefense and Emerging Infections research repository (www.beiresources.org; recombinant HA from A/Indonesia/05/2005 [H5N1]). A/Brevig Mission/1/1918 (H1N1) was purchased from Sino Biological.

ELISPOT assay. Direct ELISPOT to enumerate the number of either total IgG-secreting, pandemic H1N1 influenza–specific, or vaccine-specific plasmablasts present in the PBMC samples were essentially done as previously described (Crotty et al., 2003). In brief, 96-well ELISPOT filter plates (Millipore) were coated overnight with either the optimized amounts of purified pandemic H1N1 virions, recombinant HA from the pandemic H1N1 (as above), the 08/09 influenza vaccine at a dilution of 1/20 in PBS, or goat anti–human Ig (Invitrogen). Plates were washed and blocked by incubation with RPMI containing 10% FCS at 37°C for 2 h. Purified and extensively washed PBMCs or sorted plasmablasts were added to the plates in dilution series and incubated for 6 h. Plates were washed with PBS, followed by PBS containing 0.05% Tween, and then incubated with a biotinylated anti-huIgG (γ) antibody (Invitrogen) and incubated for 1.5 h at room temperature. After washing, the plates were incubated with an avidin-D-HRP conjugate (Vector Laboratories) and, finally, developed using AEC substrate (3 amino-9 ethylcarbazole; Sigma-Aldrich). Developed plates were scanned and analyzed using an automated ELISPOT counter (Cellular Technologies, Ltd.).

Flow cytometry analysis and cell sorting. Analytical flow cytometry analysis was performed on whole blood after lysis of erythrocytes and fixing in 2% PFA. All live cell sorting and single cell sorting was performed on purified PBMCs using either a FACSVantage or ARIAII cell sorter system. All of the following antibodies for both analytical and cell sorting cytometry were purchased from BD, except anti-CD27, which was purchased from eBioscience: anti–CD3-PECy7 or PerCP, anti–CD20-PECy7 or PerCP, anti–CD38-PE, anti–CD27-APC, and anti–CD19-FITC. ASCs were gated and isolated as $CD19^+CD3^-CD20^{lo/-}CD27^{high}$ $CD38^{high}$ cells. Flow cytometry data were analyzed using FlowJo software.

Generation of mAbs. Identification of antibody variable region genes were done essentially as previously described (Smith et al., 2009; Wardemann et al., 2003; Wrammert et al., 2008). In brief, single ASCs were sorted into 96-well PCR plates containing RNase inhibitor (Promega). VH and Vκ genes from each cell were amplified by RT-PCR and nested PCR reactions using cocktails of primers specific for both IgG and IgA using primer sets detailed in (Smith et al., 2009) and then sequenced. To generate recombinant antibodies, restriction sites were incorporated by PCR with primers to the particular variable and junctional genes. VH or Vκ genes amplified from each single cell were cloned into IgG1 or Igκ expression vectors, as previously described (Wardemann et al., 2003; Wrammert et al., 2008; Smith et al., 2009). Antibody sequences are deposited on GenBank (accession nos. HQ689701-HQ689792 available from GenBank/EMBL/DDBJ). Heavy/light chain plasmids were cotransfected into the 293A cell line for expression and antibodies purified with protein a sepharose. Antibody proteins generated in this study can be provided in limited quantities upon request.

Mutational analysis. Antibody anti-H1N1 induced plasmablast variable genes were amplified by single-cell RT-PCR using primer sets and PCR conditions that were previously published (Wrammert et al., 2008; Smith et al., 2009). Variable genes were determined using in-house analysis software compared with the Immunogentics V gene dataset and the IMGT search engine (Ehrenmann et al., 2010; Lefranc et al., 2009). Background mutation rates by this method is ∼1 base-exchange per 1,000 bases sequenced (based on sequences of constant region gene segments). Comparisons were made to historical data, some of which was previously published (Zheng et al., 2005; Wrammert et al., 2008; Duty et al., 2009).

Plaque assay and $PRNT_{50}$ assay. MDCK cells were grown in 6-well plates at a density of 8×10^5/well. On the next day, cells were washed with PBS. 10-fold dilutions of virus were added in 500 µl DME and incubated at 37°C for 1 h, with mixing every 10 min. Cells were washed with PBS and overlayed with 199 media containing 0.5% agarose (Seakem), 1x antibiotics (100 U/ml penicillin and 100 mg/ml streptomycin), 0.2% BSA (Sigma-Aldrich), and 0.5 µg/ml TPCK-Trypsin (Sigma-Aldrich). Cells were incubated for 36–40 h and fixed with 2% PFA for 10 min. Agarose plugs were removed and cells were stained with 0.1% crystal violet in 25% EtOH for 1 min. After removal from the crystal violet solution, plates were dried and used to count plaques in each well. For $PRNT_{50}$ assay, MDCK cells were prepared as above. On the next day, mAbs were threefold-diluted (60–0.74 µg/ml). 100 PFU of virus in 250 µl DME were incubated with equal volume of diluted mAbs at 37°C for 1 h before the plaque assay. Plaques were counted and the final concentration of antibodies that reduced plaques to <50 PFU were scored as $PRNT_{50}$.

Determination of 50% tissue culture infectious dose (TCID50) and MN. To determine the $TCID_{50}$, MDCK cells were grown in 96-well plate at a density of 1.5×10^4/well. On the next day, cells were washed with PBS and 10-fold diluted viruses in 100 µl DME were added into each well and incubated at 37°C for 1 h. After the incubation, cells were washed with PBS and 100 µl of DME containing 1x antibiotics (100 U/ml penicillin and 100 mg/ml streptomycin), 0.5% BSA (Sigma-Aldrich), and 0.5 µg/ml TPCK-Trypsin (Sigma-Aldrich) was added. Cells were further incubated for 60 h, and 50 µl of the supernatant was incubated with equal volume of 0.5% of PBS-washed Turkey red blood cells (Rockland Immunochemicals) for 30 min. Four replicates were performed for each dilution, and complete agglutination was scored as HA^+. Virus titers were calculated by the Reed-Muench method. For MN assay, 100 $TCID_{50}$ of virus in 50 µl DME were incubated with 50 µl of threefold-diluted antibodies (60–0.082 µg/ml) at 37°C for 1 h. Cells were washed and incubated in the media as described for the HAI assay for 60 h. The MN titer was determined to be the final concentration of mAbs that completely inhibited infection.

HAI and ELISA assays. Whole virus, recombinant HA, or vaccine-specific ELISA was performed on starting concentrations of 10 µg/ml of virus or recombinant HA and on 1:20 dilution of the vaccine, as previously described (Wrammert et al., 2008). In brief, microtiter plates were coated with live virus strains totaling 8 HAU of total virus per well or with 1 µg/ml of recombinant HA protein. To standardize the various ELISA assays, common high-affinity antibodies with similar affinities and binding characteristics against each virus strain were included on each plate, and the plate developed when the absorbance of these controls reached 3.0 ± 0.1 OD units. Goat anti–human IgG (goat anti–human I-peroxidase-conjugate; Jackson ImmunoResearch Laboratories) was used to detect binding of the recombinant antibodies, followed by development with horseradish peroxidase substrate (Bio-Rad laboratories). Absorbencies were measured at OD415 on a microplate reader (Invitrogen). Affinity estimates were calculated by nonlinear regression analysis of curves from eight dilutions of antibody (10 to 0.125 ug/ml) using GraphPad Prism. The HAI titers were determined as previously described (Wrammert et al., 2008). In brief, the samples were then serially diluted with PBS in 96- well v-bottom plates and 8 HAU (as determined by incubation with 0.5% turkey RBCs in the absence of serum) of live, egg-grown virus was added to the well. After 30 min at room temperature, 50 µl of 0.5% turkey RBCs

(Rockland Immunochemicals) suspended in PBS with 0.5% BSA was added to each well and the plates were shaken manually. After an additional 30 min at room temperature, the serum titers or minimum effective concentrations were read based on the final dilution for which a button was observed.

Competition ELISA. Competition ELISA was performed by inhibiting binding of each biotinylated antibody (NHS-coupled; Thermo Fisher Scientific) at the half-maximal binding concentration with a 10-fold molar excess of purified antibody. All comparisons of different antibodies were based on percentage of absorbance values for each antibody against itself (which was scored as 100% inhibition). Detection was done using streptavidin-HRP as described for the ELISA assay.

FACS analysis of binding of anti-HA antibodies with H5 and its mutants. The full-length HA gene (H5-TH04) of A/Thailand/2(SP-33)/2004 (H5N1) were codon-optimized for eukaryotic cell expression and cloned into pcDNA3.1 vector to obtain the pcDNA3.1-H5-TH04 construct (Sui et al., 2009). All mutants of H5-TH04 were derived from pcDNA3.1-H5-TH04 and constructed by the QuikChange method (Stratagene). The full-length wild type H5-TH04 and mutants expressing plasmids were transfected transiently into 293T cells with Lipofectamine 2000 (Invitrogen). 24 h after transfection, cells were harvested for immunostaining. Anti-HA antibodies, a control human mAb 80R (Sui et al., 2004) at 10 μg/ml, or ferret anti-H5N1 serum at 1:300 dilution were incubated with transfected 293T cells at 4°C for 1 h. Cells were then washed three times with PBS containing 0.5% BSA and 0.02% NaN_3. FITC-labeled goat anti–human IgG (Thermo Fisher Scientific) or FITC-labeled goat anti–ferret IgG (Bethyl) were then added to cells and incubated for 30 min at 4°C. Cells were washed as above, and binding of antibodies to cells was analyzed using a BD FACSCalibur with CellQuest software.

BIACORE analysis. The kinetic interactions of the mAbs with recombinant A/Cal/04/09 (H1N1) HA protein were determined by surface plasmon resonance (SPR) using a BIAcore3000 instrument. EM4CO4 and SF1009-3FO1 antibodies were immobilized at 10 $\mu l/min^{-1}$ on a CM5 sensor chip by amine coupling and recombinant HA at concentrations ranging from 0.5 to 15 nM in HBS-EP buffer were injected at 20 $\mu l/min^{-1}$ over the immobilized antibodies or reference cell surface. Running buffer (HBS-EP) was then applied for 600 s, after which the sensor surface was regenerated by a single injection of 25 mM NaOH at 100 $\mu l/min^{-1}$. For the other experiments, recombinant HA (His-tagged) was immobilized at 5 $\mu l/min^{-1}$ on NTA sensor chips with a target density of 350 response units, and the antibodies at concentrations ranging from 1 to 30 nM in HBS-P buffer were injected at 20 $\mu l/min^{-1}$ over the immobilized recombinant HA or reference cell surface, followed by a 600s dissociation phase. All experiments were performed in triplicates. For kinetic analysis, injections over reference cell surface and injections with buffer were subtracted from the data. Association rates (k_a), dissociation rates (k_d) and equilibrium dissociation constants (K_d) were calculated by aligning the curves to fit a 1:1 binding model using BIAevaluation 4.1 software. Antibodies 1009-3B06, 1000-3E01, and 1000-2G06 could not be determined because these mAbs did not bind to the recombinant HA protein from baculovirus sufficiently well for SPR. Avidities for these mAbs and for the antibodies that did not neutralize infection in vitro were estimated by Scatchard plot analyses of ELISA data (shown in parentheses).

In vivo protection experiments. 6–8-wk-old female BALB/c mice were used for the challenge studies. Mice were inoculated intranasally with 3xLD50 of a highly pathogenic, mouse-adapted pandemic H1N1 influenza virus (A/California/04/09), or PR/8/34 or FM/1/47 influenza virus. The mouse adapted pandemic H1N1 virus had been serially passaged in mice for five generations before use herein. The LD50 for all the viruses was determined by in vivo infection at various virus concentrations, according to the method of Reed and Muench. The experiments were conducted in accordance with ethical procedures and policies approved by the Emory University's Institutional Animal Care and Use Committee. To determine the prophylactic efficacy of the mAb, mice were treated intraperitoneally with 200 μg (10 mg/kg of body weight) of the specific mAbs. 12 h later, mice were challenged with 3xLD50 of one of the mouse adapted influenza viruses used in the study. All mice were monitored daily for any signs of morbidity and mortality. Body weight changes were registered daily for a period of 14 d. All mice that lost >25% of their initial body weight were sacrificed according to the institutional animal care and use committee guidelines. To determine the therapeutic efficacy of the mAbs, mice were challenged with 3xLD50 of the mouse-adapted pandemic H1N1 virus. At various times after infection (12, 24, 36, 48, 60, and 72 h) mice were treated intraperitoneally with 200 μg (10 mg/kg of body weight) of the specific mAbs. All mice were monitored daily and the body weight changes were registered daily as described above.

Statistical analysis. Data were collected and graphed using MS Excel and GraphPad Prism software. Efficacy of the therapeutic and challenge experiments was evaluated by analysis of variance using GraphPad Prism software.

Online supplemental material. Fig. S1 shows the binding characteristics of control mAbs. Fig. S2 shows further binding characteristics of the neutralizing mAbs. Fig. S3 shows further analysis of pandemic H1N1-induced plasmablast somatic mutations. Fig. S4 shows experiments demonstrating the therapeutic control of pandemic H1N1 viral titers in lungs after mAb treatment. Tables S1–S3 provide detailed characteristics concerning the variable gene sequences cloned from pandemic H1N1 induced plasmablasts. Online supplemental material is available at http://www.jem.org/cgi/content/full/jem.20101352/DC1.

We thank Drs. Richard J. Webby and Gillian Air for providing us with viral isolates. We also thank Robert Karaffa and Sommer Durham for providing essential support with cell sorting and Dr. Ruben Donis (CDC) for his generous gift of ferret anti-H5 serum.

This work was funded in parts by National Institutes of Health (NIH)/National Institute of Allergy and Infectious Diseases (NIAID) U19-AI057266 with ARRA supplement funding U19 AI057266-06S2 (R. Ahmed and P.C. Wilson), by NIH/NIAID HHSN266200700006C Center of Excellence for Influenza Research and Surveillance (R. Ahmed, R. Compans, and P.C. Wilson), by the Northeast Biodefense Center U54-AI057158-Lipkin (R. Ahmed, W.I. Lipkin, and P.C. Wilson), by NIH/NIAID HHSN266200500026C (P.C. Wilson), by NIH/NIAID 5U19AI062629-05 (P.C. Wilson), and by NIH/NIAID U01 AI074518 (W.A. Marasco) and the National Foundation for Cancer Research (W.A.M.). J. Wrammert was supported by a training fellowship through the Center of Excellence for Influenza Research and Surveillance and D. Koutsonanos by U01-AI074579 (R. Compans). This research was supported in part by the Intramural Research Program of the NIAID.

The authors declare no financial or commercial conflicts of interest.

Submitted: 6 July 2010
Accepted: 13 December 2010

REFERENCES

Beigel, J.H. 2008. Influenza. *Crit. Care Med.* 36:2660–2666. doi:10.1097/CCM.0b013e318180b039

Bernasconi, N.L., E. Traggiai, and A. Lanzavecchia. 2002. Maintenance of serological memory by polyclonal activation of human memory B cells. *Science.* 298:2199–2202. doi:10.1126/science.1076071

Brockwell-Staats, C., R.G. Webster, and R.J. Webby. 2009. Diversity of Influenza Viruses in Swine and the Emergence of a Novel Human Pandemic Influenza A (H1N1). *Influenza Other Respir. Viruses.* 3:207–213. doi:10.1111/j.1750-2659.2009.00096.x

Brokstad, K.A., R.J. Cox, J. Olofsson, R. Jonsson, and L.R. Haaheim. 1995. Parenteral influenza vaccination induces a rapid systemic and local immune response. *J. Infect. Dis.* 171:198–203.

Corti, D., A.L. Suguitan Jr., D. Pinna, C. Silacci, B.M. Fernandez-Rodriguez, F. Vanzetta, C. Santos, C.J. Luke, F.J. Torres-Velez, N.J. Temperton, et al. 2010. Heterosubtypic neutralizing antibodies are produced by individuals immunized with a seasonal influenza vaccine. *J. Clin. Invest.* 120:1663–1673.

Crotty, S., P. Felgner, H. Davies, J. Glidewell, L. Villarreal, and R. Ahmed. 2003. Cutting edge: long-term B cell memory in humans after smallpox vaccination. *J. Immunol.* 171:4969–4973.

Dawood, F.S., S. Jain, L. Finelli, M.W. Shaw, S. Lindstrom, R.J. Garten, L.V. Gubareva, X. Xu, C.B. Bridges, and T.M. Uyeki; Novel Swine-Origin Influenza A (H1N1) Virus Investigation Team. 2009. Emergence of a novel swine-origin influenza A (H1N1) virus in humans. *N. Engl. J. Med.* 360:2605–2615. doi:10.1056/NEJMoa0903810

de Wildt, R.M., I.M. Tomlinson, W.J. van Venrooij, G. Winter, and R.M. Hoet. 2000. Comparable heavy and light chain pairings in normal and systemic lupus erythematosus IgG(+) B cells. *Eur. J. Immunol.* 30: 254–261. doi:10.1002/1521-4141(200001)30:1<254::AID-IMMU254>3.0.CO;2-X

Duty, J.A., P. Szodoray, N.Y. Zheng, K.A. Koelsch, Q. Zhang, M. Swiatkowski, M. Mathias, L. Garman, C. Helms, B. Nakken, et al. 2009. Functional anergy in a subpopulation of naive B cells from healthy humans that express autoreactive immunoglobulin receptors. *J. Exp. Med.* 206:139–151. doi:10.1084/jem.20080611

Ehrenmann, F., Q. Kaas, and M.P. Lefranc. 2010. IMGT/3Dstructure-DB and IMGT/DomainGapAlign: a database and a tool for immunoglobulins or antibodies, T cell receptors, MHC, IgSF and MhcSF. *Nucleic Acids Res.* 38(Database issue):D301–D307. doi:10.1093/nar/gkp946

Ekiert, D.C., G. Bhabha, M.A. Elsliger, R.H. Friesen, M. Jongeneelen, M. Throsby, J. Goudsmit, and I.A. Wilson. 2009. Antibody recognition of a highly conserved influenza virus epitope. *Science.* 324:246–251. doi:10.1126/science.1171491

Garten, R.J., C.T. Davis, C.A. Russell, B. Shu, S. Lindstrom, A. Balish, W.M. Sessions, X. Xu, E. Skepner, V. Deyde, et al. 2009. Antigenic and genetic characteristics of swine-origin 2009 A(H1N1) influenza viruses circulating in humans. *Science.* 325:197–201. doi:10.1126/science.1176225

Gerhard, W., K. Mozdzanowska, M. Furchner, G. Washko, and K. Maiese. 1997. Role of the B-cell response in recovery of mice from primary influenza virus infection. *Immunol. Rev.* 159:95–103. doi:10.1111/j.1600-065X.1997.tb01009.x

Hancock, K., V. Veguilla, X. Lu, W. Zhong, E.N. Butler, H. Sun, F. Liu, L. Dong, J.R. DeVos, P.M. Gargiullo, et al. 2009. Cross-reactive antibody responses to the 2009 pandemic H1N1 influenza virus. *N. Engl. J. Med.* 361:1945–1952. doi:10.1056/NEJMoa0906453

Koelsch, K., N.-Y. Zheng, Q. Zhang, A. Duty, C. Helms, M.D. Mathias, M. Jared, K. Smith, J.D. Capra, and P.C. Wilson. 2007. Mature B cells class switched to IgD are autoreactive in healthy individuals. *J. Clin. Invest.* 117:1558–1565. doi:10.1172/JCI27628

Krause, J.C., T.M. Tumpey, C.J. Huffman, P.A. McGraw, M.B. Pearce, T. Tsibane, R. Hai, C.F. Basler, and J.E. Crowe Jr. 2010. Naturally occurring human monoclonal antibodies neutralize both 1918 and 2009 pandemic influenza A (H1N1) viruses. *J. Virol.* 84:3127–3130. doi:10.1128/JVI.02184-09

Lefranc, M.P., V. Giudicelli, C. Ginestoux, J. Jabado-Michaloud, G. Folch, F. Bellahcene, Y. Wu, E. Gemrot, X. Brochet, J. Lane, et al. 2009. IMGT, the international ImMunoGeneTics information system. *Nucleic Acids Res.* 37(Database issue):D1006–D1012. doi:10.1093/nar/gkn838

Luke, T.C., E.M. Kilbane, J.L. Jackson, and S.L. Hoffman. 2006. Meta-analysis: convalescent blood products for Spanish influenza pneumonia: a future H5N1 treatment? *Ann. Intern. Med.* 145:599–609.

Manicassamy, B., R.A. Medina, R. Hai, T. Tsibane, S. Stertz, E. Nistal-Villán, P. Palese, C.F. Basler, and A. García-Sastre. 2010. Protection of mice against lethal challenge with 2009 H1N1 influenza A virus by 1918-like and classical swine H1N1 based vaccines. *PLoS Pathog.* 6:e1000745. doi:10.1371/journal.ppat.1000745

McKean, D., K. Huppi, M. Bell, L. Staudt, W. Gerhard, and M. Weigert. 1984. Generation of antibody diversity in the immune response of BALB/c mice to influenza virus hemagglutinin. *Proc. Natl. Acad. Sci. USA.* 81:3180–3184. doi:10.1073/pnas.81.10.3180

Okuno, Y., Y. Isegawa, F. Sasao, and S. Ueda. 1993. A common neutralizing epitope conserved between the hemagglutinins of influenza A virus H1 and H2 strains. *J. Virol.* 67:2552–2558.

Palladino, G., K. Mozdzanowska, G. Washko, and W. Gerhard. 1995. Virus-neutralizing antibodies of immunoglobulin G (IgG) but not of IgM or IgA isotypes can cure influenza virus pneumonia in SCID mice. *J. Virol.* 69:2075–2081.

Puck, J.M., W.P. Glezen, A.L. Frank, and H.R. Six. 1980. Protection of infants from infection with influenza A virus by transplacentally acquired antibody. *J. Infect. Dis.* 142:844–849.

Renegar, K.B., P.A. Small Jr., L.G. Boykins, and P.F. Wright. 2004. Role of IgA versus IgG in the control of influenza viral infection in the murine respiratory tract. *J. Immunol.* 173:1978–1986.

Reuman, P.D., C.M. Paganini, E.M. Ayoub, and P.A. Small Jr. 1983. Maternal-infant transfer of influenza-specific immunity in the mouse. *J. Immunol.* 130:932–936.

Sasaki, S., M.C. Jaimes, T.H. Holmes, C.L. Dekker, K. Mahmood, G.W. Kemble, A.M. Arvin, and H.B. Greenberg. 2007. Comparison of the influenza virus-specific effector and memory B-cell responses to immunization of children and adults with live attenuated or inactivated influenza virus vaccines. *J. Virol.* 81:215–228. doi:10.1128/JVI.01957-06

Simmons, C.P., N.L. Bernasconi, A.L. Suguitan, K. Mills, J.M. Ward, N.V.V. Chau, T.T. Hien, F. Sallusto, Q. Ha, J. Farrar, et al. 2007. Prophylactic and therapeutic efficacy of human monoclonal antibodies against H5N1 influenza. *PLoS Med.* 4:e178. doi:10.1371/journal.pmed.0040178

Smith, K., L. Garman, J. Wrammert, N.Y. Zheng, J.D. Capra, R. Ahmed, and P.C. Wilson. 2009. Rapid generation of fully human monoclonal antibodies specific to a vaccinating antigen. *Nat. Protoc.* 4:372–384. doi:10.1038/nprot.2009.3

Steel, J., A.C. Lowen, T. Wang, M. Yondola, Q. Gao, K. Haye, A. Garcia-Sastre, and P. Palese. 2010. Influenza virus vaccine based on the conserved hemagglutinin stalk domain. *MBio.* 1:e00018-10.

Subbarao, K. and T. Joseph. 2007. Scientific barriers to developing vaccines against avian influenza viruses. *Nat. Rev. Immunol.* 7:267–278.

Sui, J., W. Li, A. Murakami, A. Tamin, L.J. Matthews, S.K. Wong, M.J. Moore, A.S. Tallarico, M. Olurinde, H. Choe, et al. 2004. Potent neutralization of severe acute respiratory syndrome (SARS) coronavirus by a human mAb to S1 protein that blocks receptor association. *Proc. Natl. Acad. Sci. USA.* 101:2536–2541. doi:10.1073/pnas.0307140101

Sui, J., W.C. Hwang, S. Perez, G. Wei, D. Aird, L.M. Chen, E. Santelli, B. Stec, G. Cadwell, M. Ali, et al. 2009. Structural and functional bases for broad-spectrum neutralization of avian and human influenza A viruses. *Nat. Struct. Mol. Biol.* 16:265–273. doi:10.1038/nsmb.1566

Sweet, C., R.A. Bird, K. Jakeman, D.M. Coates, and H. Smith. 1987. Production of passive immunity in neonatal ferrets following maternal vaccination with killed influenza A virus vaccines. *Immunology.* 60:83–89.

Wang, T.T., G.S. Tan, R. Hai, N. Pica, E. Petersen, T.M. Moran, and P. Palese. 2010. Broadly protective monoclonal antibodies against H3 influenza viruses following sequential immunization with different hemagglutinins. *PLoS Pathog.* 6:e1000796. doi:10.1371/journal.ppat.1000796

Wardemann, H., S. Yurasov, A. Schaefer, J.W. Young, E. Meffre, and M.C. Nussenzweig. 2003. Predominant autoantibody production by early human B cell precursors. *Science.* 301:1374–1377. doi:10.1126/science.1086907

Wei, C.J., J.C. Boyington, P.M. McTamney, W.P. Kong, M.B. Pearce, L. Xu, H. Andersen, S. Rao, T.M. Tumpey, Z.Y. Yang, and G.J. Nabel. 2010. Induction of broadly neutralizing H1N1 influenza antibodies by vaccination. *Science.* 329:1060–1064. doi:10.1126/science.1192517

Wrammert, J., K. Smith, J. Miller, W.A. Langley, K. Kokko, C. Larsen, N.Y. Zheng, I. Mays, L. Garman, C. Helms, et al. 2008. Rapid cloning of high-affinity human monoclonal antibodies against influenza virus. *Nature.* 453:667–671. doi:10.1038/nature06890

Xu, R., D.C. Ekiert, J.C. Krause, R. Hai, J.E. Crowe Jr., and I.A. Wilson. 2010. Structural basis of preexisting immunity to the 2009 H1N1 pandemic influenza virus. *Science.* 328:357–360.

Zheng, N.Y., K. Wilson, X. Wang, A. Boston, G. Kolar, S.M. Jackson, Y.J. Liu, V. Pascual, J.D. Capra, and P.C. Wilson. 2004. Human immunoglobulin selection associated with class switch and possible tolerogenic origins for C delta class-switched B cells. *J. Clin. Invest.* 113:1188–1201.

Zheng, N.Y., K. Wilson, M. Jared, and P.C. Wilson. 2005. Intricate targeting of immunoglobulin somatic hypermutation maximizes the efficiency of affinity maturation. *J. Exp. Med.* 201:1467–1478. doi:10.1084/jem.20042483